

## *Helicobacter pylori* NikR's Interaction with DNA: A Two-Tiered Mode of Recognition<sup>†</sup>

Nuvjeevan S. Dosanjh, Abby L. West, and Sarah L. J. Michel\*

Department of Pharmaceutical Sciences, School of Pharmacy, University of Maryland, Baltimore, Maryland 21201-1180

Received August 6, 2008; Revised Manuscript Received November 21, 2008

**ABSTRACT:** *HPNikR* is a prokaryotic nickel binding transcription factor found in the virulent bacterium *Helicobacter pylori*. *HPNikR* regulates the expression of multiple genes as an activator or repressor, including those involved in nickel ion homeostasis, acid adaptation, and iron uptake. The target operator sequences of the genes regulated by *HPNikR* do not contain identifiable symmetrical recognition sites, and the mechanism by which *HPNikR* distinguishes between the genes it regulates is not understood. Using competitive fluorescence anisotropy (FA) and electrophoretic gel mobility shift (EMSA) assays, the interactions between *HPNikR* and the target operator sequences of the genes directly regulated (*ureA*, *NixA*, *NikR*, *Fur OPI*, *Fur OPII*, *Frbp4*, *FecA3*, and *exbB*) were characterized. These studies revealed that *HPNikR* utilizes a two-tiered mode of DNA recognition by binding to some genes with high affinity and others with low affinity. The genes that are tightly regulated by *HPNikR* encode proteins that utilize nickel, while those that are less tightly regulated encode other types of proteins. The affinities of low-affinity metal ions for a second metal binding site were determined to be in the micromolar regime, and a contribution of electrostatics to the *HPNikR*–DNA binding event was determined. Detailed studies of the role of sequence length and identity for the interaction between *HPNikR* and *ureA* revealed a specific length requirement for DNA binding.

*Helicobacter pylori* (HP)<sup>1</sup> is a virulent pathogen that colonizes the gastric epithelium of humans, leading to gastric ulcers in the short term and several types of gastric cancers over the long term (1–4). More than half of the world's population is infected by *H. pylori*, making it a significant public health threat (5), and there is a documented need for the development of novel anti-*Helicobacter* agents to target this pathogen (5). Typically, the pH in the gastric epithelium ranges from 4 to 6.5 with periodic acid shocks of pH <2 (6, 7). To survive under these conditions, *H. pylori* utilizes urease, a nickel cofactor metalloenzyme, which converts urea to ammonia and bicarbonate to neutralize its local environment (8–10).

Although nickel is required for *H. pylori* survival, it can be toxic at high concentrations (11). As a result, *H. pylori*

must tightly control intracellular nickel levels (12–15). Often, organisms use specific metalloregulatory proteins to maintain intracellular metal ion homeostasis (16–18). A key protein involved in nickel ion metabolism and homeostasis for *H. pylori* is the nickel regulatory protein, NikR (12, 13). *HPNikR* regulates multiple genes as an activator or repressor by binding to varied operator sequences (14, 19–25). Interestingly, these genes include both genes that encode proteins that utilize nickel to function, such as *NixA* (a nickel importer), *HPN* (a nickel storage protein), and *UreA* (urease), and genes that encode proteins that do not directly use nickel, such as genes involved in iron uptake and storage (e.g., *pfr* and *fur*), genes involved in motility (e.g., *cheV*, *flaA*, and *flab*), genes involved in stress response (e.g., *hrcA*, *grpE*, and *dnaK*), and genes that encode outer membrane proteins (e.g., *omp11*, *omp31*, and *omp32*) (12). The *H. pylori* genome was sequenced in 1997 and found to be significantly smaller than other prokaryotic genomes, such as that of *Escherichia coli* (EC) (26). *HPNikR* represents one of the few global regulators of gene expression in *H. pylori* and because of the comparatively small size of its genome has acquired multiple functions (27).

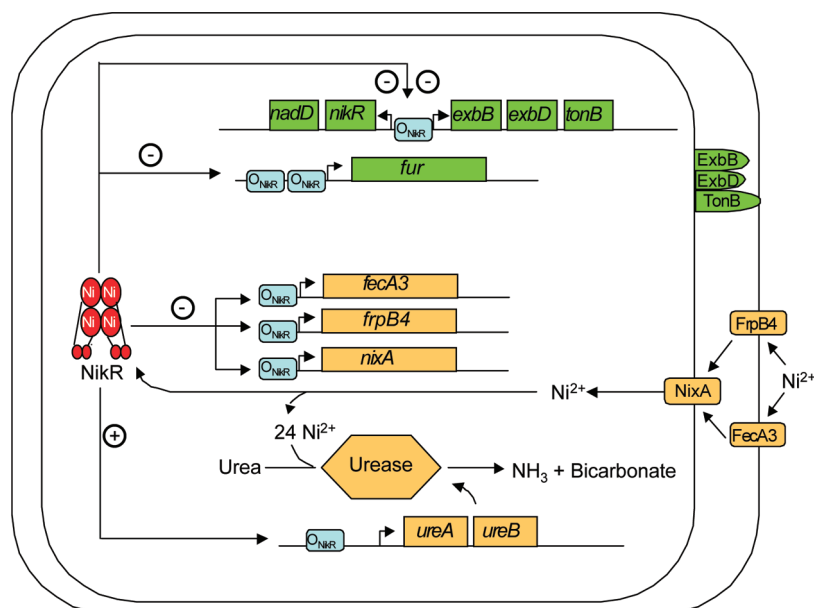
The evidence for the regulation of multiple genes by *HPNikR* comes primarily from transcriptional profiling studies of up- and downregulated genes by *HPNikR* and nickel (27). These studies are limited in their capacity to distinguish between genes that are regulated directly by *HPNikR* and those that

<sup>†</sup> We are grateful to the University of Maryland Baltimore for support of this research.

\* To whom correspondence should be addressed. Phone: (410) 706-7038. Fax: (410) 706-5017. E-mail: smichel@rx.umaryland.edu.

<sup>1</sup> Abbreviations: DEPC, diethyl pyrocarbonate; DTT, dithiothreitol; EC, *E. coli*; EDTA, ethylenediaminetetraacetic acid; FA, fluorescence anisotropy;  $F_{\text{bound}}$ , fraction bound; F, fluorescein; FPLC, fast protein liquid chromatography; HEPES, 4-(2-hydroxyethyl)-1-piperazineethanesulfonic acid; HP, *H. pylori*; IPTG, isopropyl  $\beta$ -D-thiogalactopyranoside;  $K_d$ , dissociation constant; LB, Luria-Bertani; MALDI-TOF, matrix-assisted laser desorption ionization time-of-flight; MES, 2-(*N*-morpholino)ethanesulfonic acid; PCR, polymerase chain reaction;  $r$ , anisotropy; SDS–PAGE, sodium dodecyl sulfate–polyacrylamide gel electrophoresis; TRIS, tris(hydroxymethyl)aminomethane.

Scheme 1



utilize an accessory pathway. A small subset of the *HPNikR*-regulated genes has been studied in more detail in vitro using DNase footprinting studies. From these studies, seven genes were shown to be directly regulated by *HPNikR*. These genes include *ureA* which encodes urease (19, 20, 22, 24), *nixA* which encodes a high-affinity inner membrane nickel transporter (20, 24), *exbB* which is part of the TonB-ExbBD complex which provides energy for nickel and iron uptake (22), *fur* which encodes the ferric uptake regulator (the other metallotranscription factor identified in *H. pylori*) (22), *fecA3* and *frpB4* which are outer membrane nickel transporters (25), and *nikR* which encodes NikR (22). Scheme 1 provides an overview of the regulation of these genes by *HPNikR*. *HPNikR* activates *ureA* transcription and represses *nixA*, *exbB*, *fecA3*, and *frpB4* transcription, and its regulatory role for *fur* has not been defined.

The recognition sequences of the genes directly regulated by *HPNikR* differ, although a putative palindrome ("NikR Box" sequence) that is required for recognition has been proposed by aligning the recognition sequences. The palindrome is AT rich and contains an 11 base pair linker (22). None of the proposed recognition sites for the genes regulated by *HPNikR* are symmetrical. We hypothesized that this perceptible asymmetry may allow *HPNikR* to bind to multiple asymmetric sequences with varied affinities as part of the mechanism of multi-DNA regulation by *HPNikR*.

The only homologue of *HPNikR* for which a DNA recognition sequence has been identified is from *E. coli*. Only one function has been ascribed to *ECNikR*, repression of NikABCDE, a nickel transporter (13, 28–30). This promoter's recognition sequence is completely different from that identified for *HPNikR* in both sequence and length, suggesting that *HPNikR* may recognize DNA in a manner different from that of *ECNikR*. The unique ability of *HPNikR* to directly recognize multiple genes of varied sequences raises the question of how *HPNikR* distinguishes between the different genes it controls. We hypothesize that the protein uses differential binding affinities to distinguish between the genes it regulates. Using a previously developed fluorescence anisotropy-based DNA binding assay, we have tested this hypothesis in the work reported here (23).

Surprisingly, we have discovered that *HPNikR* shows either tight or weak binding to the genes it regulates, and we now propose that a two-tiered DNA recognition mechanism is operative for *HPNikR*.

## EXPERIMENTAL PROCEDURES

**Protein Expression and Purification.** The pET15b construct containing *HPNikR* was transformed into *E. coli* BL21(DE3) cells (1 L for large-scale expression) and grown in LB medium containing 100 µg/mL ampicillin. Purification of *HPNikR* was carried out using a nickel-loaded 5 mL Hitrap-HP (Amersham) affinity column followed by further purification using a Hitrap Q-Sepharose (Amersham) column as previously described (23). MALDI MS was used to confirm the molecular weight (expected, 17147.2; observed, 17147.2). Approximately 30–40 mg of *HPNikR* is obtained from a starting culture of 1 L. Because *HPNikR* has several cysteine residues, all further manipulations were carried out anaerobically using a Coy inert atmospheric chamber (95% N<sub>2</sub> and 5% H<sub>2</sub>) to prevent cysteine oxidation.

**Generation of Apo-HPNikR.** Apo-*HPNikR* was prepared by incubation of the protein with 50 mM EDTA and 10 mM DTT overnight at 35 °C followed by exhaustive dialysis with 20 mM Hepes, 100 mM NaCl Chelex-treated buffer at pH 7.5. The dialyzed protein was then buffer exchanged and concentrated using a centricon-plus 20 device (Millipore) against a Chelex-prepared 20 mM Hepes, 100 mM NaCl, 20 mM glycine buffer at pH 7.5.

**Oligonucleotide Probes.** HPLC-purified oligonucleotides were purchased from Operon either labeled with fluorescein (F) or unlabeled and are shown in Table 1.

Upon receipt, the oligonucleotides were resuspended in DNase-free water and quantified. For annealing, each oligonucleotide was mixed such that there was a 1.25:1 ratio of unlabeled to labeled oligonucleotide in 10 mM Tris, 10 mM NaCl annealing buffer at pH 8.0. The annealing reaction mixtures were placed in a water bath set to a temperature 10 °C greater than the melting temperatures (*T<sub>m</sub>*'s) of the component oligonucleotides. The water bath was then

Table 1

Operator	Sequence (5'→3')
<i>pUreA-F</i>	CTTCAAAGATATAACACTAATT [F] CATTTTAAATAATAATTAGTTAATGAA
<i>pUreA</i>	CTTCAAAGATATAACACTAATTCATTTTAAATAATAATTAGTTAATGAA
<i>pUreA-Δpal</i>	CTTCAAAGATACCCCCCAATTCATTTTACCCCCCATTAGTTAATGAA
<i>pUreA-Δpal1</i>	CTTCAAAGATACCCCCCAATTCATTTTAAATAATAATTAGTTAATGAA
<i>pUreA-Δpal2</i>	CTTCAAAGATATAACACTAATTCATTTTACCCCCCATTAGTTAATGAA
<i>pUreA-perf</i>	CTTCAAAGATATATTATTAATTCATTTTAAATAATAATTAGTTAATGAA
<i>pUreA-32</i>	ATATAACACTAATTCATTTTAAATAATAATTA
<i>pUreA-32 GC</i>	CCATAACACTAATTCATTTTAAATAATAACCC
<i>pUreA-27</i>	ATAACACTAATTCATTTTAAATAATA
<i>pNixA</i>	AACAAAATATATTACAATTACCAAAAAAGTATTATTTTCTTAAAAGGT
<i>pFrpB4</i>	ACAAATTTAAGGTATTATTAAATAGAATAATGTAATAATAACCTTAGGT
<i>pFecA3</i>	TAAAATTCGCGACATTATTAAGTTTTTTTTGTTTTTATTACTTAATAAT
<i>pExbB</i>	TTATTGACTTGTTATTATTAAAACAATATAATCAACAAACCAACATTCC
<i>pNikR</i>	AAATCCAGTTTGTATTATAATTGTTTCATTTTAAATTAATTCATCATAC
<i>pFur-OPI</i>	TATGTTTCATCGCATTATTATTGTATAATAATATTCTAGTTATAAAAAT
<i>pFur-OPII</i>	ATAAGAAATTGATCTTATAAGTTACATTAAATGCGACAATGGTAATAA

immediately turned off, and the annealing reaction mixtures were allowed to cool overnight. Double-stranded oligonucleotides were quantified and stored at  $-20^{\circ}\text{C}$ .

**Competitive Fluorescence Anisotropy Titrations.** Measurements were taken with an ISS PC-1 spectrofluorometer configured in the L format. Initially, a full excitation and emission experiment was conducted to determine the optimal excitation and emission wavelengths for the experiment. The excitation wavelength and band-pass used in the experiments were 495 and 2 nm, respectively, and the emission wavelength and band-pass were 519 and 1 nm, respectively.

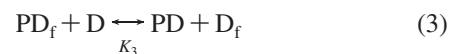
The competitive anisotropy assays were conducted in 20 mM HEPES, 100 mM NaCl, 20 mM glycine, and 3 mM  $\text{MgCl}_2$  at pH 7.5 prepared in a 0.5 cm PL Spectrosil far-UV quartz window fluorescence cuvette (Starna Cells) as previously described (23). In a typical experiment, an unlabeled DNA molecule was titrated into a solution containing 375 nM Ni(II)HPNikR (tetramer) and 15 nM *pUreA-F*, and the decrease in anisotropy ( $r$ ) as the unlabeled DNA oligomer competed with the labeled oligonucleotide was recorded. The anisotropy was converted to fraction bound, to take into account changes in quantum yield, using the following equation

$$F_{\text{bound}} = \frac{r - r_{\text{free}}}{(r_{\text{bound}} - r)Q + (r - r_{\text{free}})}$$

where  $r_{\text{free}}$  is the anisotropy of the fluorescein-labeled oligonucleotide,  $r_{\text{bound}}$  is the anisotropy of the DNA–protein

complex at saturation taken from the forward titration, and  $Q$  is the quantum yield ratio of the bound to the free form and is calculated from the fluorescence intensity changes that occur ( $Q = I_{\text{bound}}/I_{\text{free}}$ ) (31). The competition experiment was performed with Ni(II)HPNikR concentrations at levels near saturation to minimize the amount of unlabeled DNA required to complete the titration. Experiments were performed aerobically as no difference in binding was observed between experiments performed anaerobically and aerobically.

Binding isotherms were fit using Mathematica (version 5.2, Wolfram Research) to a model that involved the mass action equations for the three competing equilibria:



where P is the nickel-bound protein (HPNikR),  $\text{D}_f$  is fluorescently labeled DNA, and D represents unlabeled DNA. The value for  $K_1$  was determined from the forward titrations and thus used as a known parameter for the fit. The Mathematica software was used to combine eq 1–3 and to solve the resulting cubic equation in terms of  $\text{PD}_f$  using

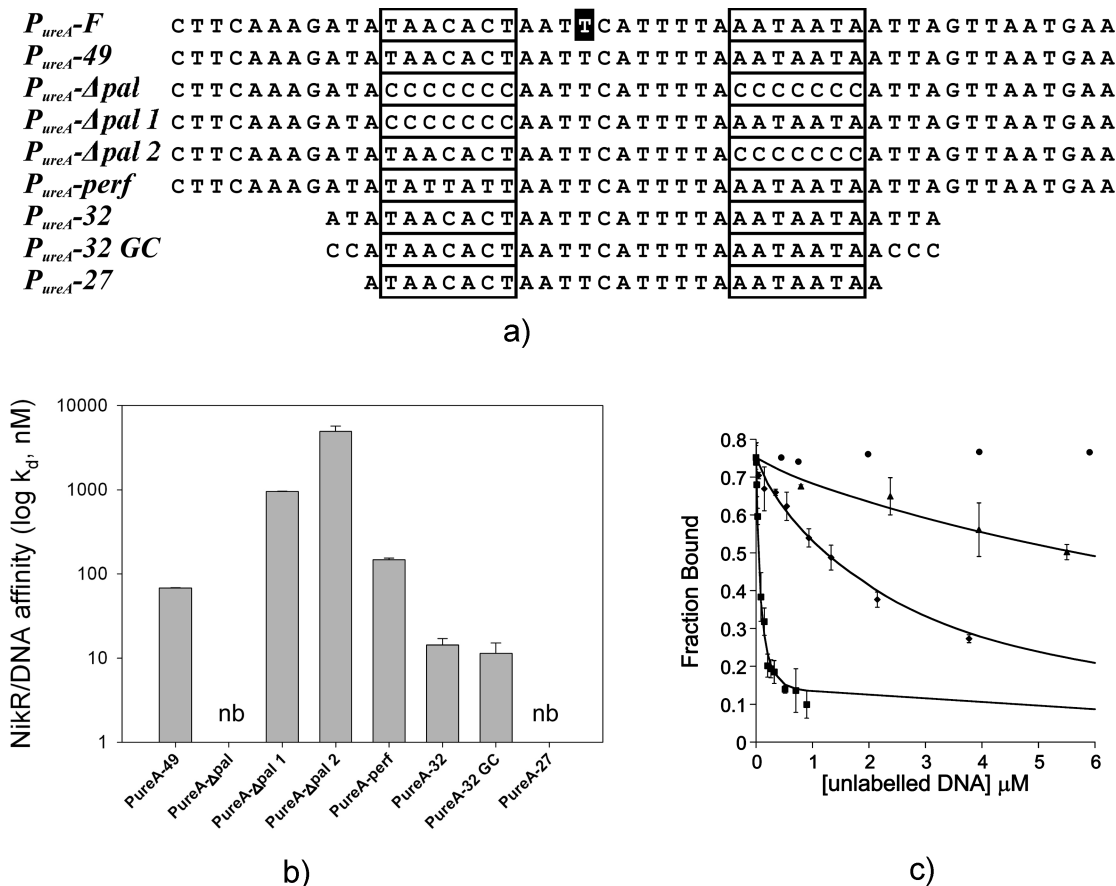
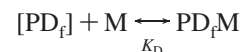


FIGURE 1: Fluorescence anisotropy-monitored binding (FA) of NiHPNikR variants of the  $P_{ureA}$  promoter. (a) Oligonucleotide sequences used in this study. The putative palindrome is boxed, and for  $P_{ureA}$ -F, the fluorescently labeled thymine is highlighted with a black background. (b) Graphical representation of determined dissociation constants in the interaction of NiHPNikR with  $P_{ureA}$  promoter variants. NB denotes no binding. (c) Competitive titration of unlabeled  $P_{ureA}$  (49mer) (■) into 15 nM  $P_{ureA}$ -F and 375 nM NikR. Titrations of sequences lacking the first palindrome,  $P_{ureA}$ - $\Delta$ pal 1 (◆), second palindrome,  $P_{ureA}$ - $\Delta$ pal 2 (▲), and a truncated 27mer,  $P_{ureA}$ -27 (●), into 5 nM  $P_{ureA}$ -F and 88 nM NikR are also shown. Data were fit to a competitive binding equilibrium and represent the average of three sets of binding data. All FA experiments were performed in 20 mM Hepes, 100 mM NaCl, 20 mM glycine, and 3 mM  $MgCl_2$  at pH 7.5 and 25 °C.

nonlinear, least-squares analysis. All titrations were carried out in triplicate.

**Salt-Dependent DNA Binding Studies.** The electrostatic contributions to binding were measured using direct fluorescence anisotropy assays for the interaction between  $[Ni(II)HPNikR]_4$  and  $pUreA$ -F and competitive fluorescence anisotropy assays for the interaction between  $[Ni(II)HPNikR]_4$  and  $pFur$  OPI. All FA studies were conducted using 20 mM HEPES, 20 mM glycine, and 3 mM  $MgCl_2$  at pH 7.5 as a buffer which was prepared in a 0.5 cm PL Spectrosil far-UV quartz window fluorescence cuvette (Starna Cells) as previously described (23). The concentration of NaCl varied from 100 to 250 mM.

**Titration of  $Mg^{2+}$ ,  $Ca^{2+}$ , and  $Mn^{2+}$  with  $[Ni(II)HPNikR]_4[P_{UreA}-F]$ .** The fluorescence anisotropy of a solution of 1  $\mu$ M  $[Ni(II)HPNikR]_4$  and 15 nM  $P_{UreA}$ -F in 20 mM Hepes, 100 mM NaCl, and 20 mM glycine in a 0.5 PL Spectrosil far-UV quartz window fluorescence cuvette (Starna Cells) was recorded. A metal salt ( $MgCl_2$ ,  $CaCl_2$ , or  $MnCl_2$ ) was then titrated, and the change in fluorescence anisotropy was monitored until saturation. Data were analyzed by converting the anisotropy,  $r$ , to fraction bound ( $F_{bound}$ ) and fitting the data to 1:1 binding model. Dissociation constants,  $K_d$ , were determined using Kaledagraph:



**Electrophoretic Mobility Shift Assay (EMSA).** All EMSAs between HPNikR and DNA were conducted using a 7% nondenaturing acrylamide gel and a TAE (Tris-acetate EDTA) running buffer containing 800  $\mu$ M  $NiSO_4$  with and without 3 mM  $MgCl_2$ . Approximately 250 nM  $pUreA$  DNA was incubated with increasing concentrations of NiHPNikR (0, 5, and 50  $\mu$ M, except for  $P_{NikR}$ ,  $P_{fur}$ -OPI, and  $P_{fur}$ -OPII operator sequences where 0, 50, and 200  $\mu$ M, respectively, were used) for 1 h at room temperature followed by electrophoresis at 4 °C and 100 V. The acrylamide gel was stained with ethidium bromide and viewed with a UV light box.

## RESULTS

**Competitive Binding Titrations of Ni(II)HPNikR with  $P_{ureA}$  Variants.** Building upon our earlier report in which we developed a competitive fluorescence anisotropy (FA) assay to quantify the binding interaction between Ni(II)HPNikR and a DNA sequence corresponding to the  $ureA$  promoter ( $P_{ureA}$ ) (23), we designed a series of  $ureA$  operator mutants, listed in Figure 1a, to test how altering either the nature of the recognition palindrome or the length of the  $ureA$



recognition sequence affects binding. For these experiments, Ni(II)HPNikR was first titrated with P<sub>ureA</sub>-F [fluorescein-conjugated *ureA* (Figure 1a)] followed by the addition of unlabeled variants of the *ureA* operator sequence and the resultant decrease in anisotropy monitored. The data were then fit to a competitive binding model.

The P<sub>ureA</sub> sequence contains an imperfect palindrome that we previously demonstrated to be required for Ni(II)HPNikR binding (boxed in Figure 1a) (23). To determine the role of each half-site of the palindrome in this binding interaction, FA titrations with P<sub>ureA</sub> oligomers in which either the first or second palindrome sequence was modified to all cytosines (P<sub>ureA-Δpal1</sub> or P<sub>ureA-Δpal2</sub>, respectively) were performed. Removal of the second palindrome had a more dramatic effect on binding affinity than removal of the first. We determined a dissociation constant of  $4.9 \pm 0.78 \mu\text{M}$  for the interaction between Ni(II)HPNikR and P<sub>ureA-Δpal2</sub>, which lacked the second palindrome, and a dissociation constant of  $1.0 \pm 0.094 \mu\text{M}$  for the interaction between Ni(II)HPNikR and P<sub>ureA-Δpal1</sub>, which lacked the first palindrome (Figure 1b,c). These studies imply that, for the *ureA* operator, the integrity of both half-sites is necessary for full Ni(II)HPNikR binding activity and that the second half-site contributes more to the binding interaction than the first. The P<sub>ureA</sub> recognition palindrome is not perfectly symmetrical, and we sought to determine if a perfect palindrome would impart tighter binding. We designed a mutant *ureA* operator fragment containing a perfect palindromic repeat, P<sub>ureA</sub>-perf, identified by aligning the HPNikR target sequences (22). P<sub>ureA</sub>-perf is 49 bp in length and contains a TATTATT-X<sub>11</sub>-AATAATA palindromic inverted repeat (Figure 1a). Surprisingly, the affinity of Ni(II)HPNikR for P<sub>ureA</sub>-perf was weaker than that of the native wild-type P<sub>ureA</sub>-49: a dissociation constant of  $143 \pm 10 \text{ nM}$  was determined for Ni(II)HPNikR with P<sub>ureA</sub>-perf compared to  $67 \pm 1.0 \text{ nM}$  for Ni(II)HPNikR with P<sub>ureA</sub>-49 (Figure 1b). This result suggests that the presence of a perfect palindromic repeat in the *ureA* operator does not confer greater binding recognition by Ni(II)HPNikR as it preferentially binds the native asymmetric *ureA* target site.

Our previous studies of the binding interaction between Ni(II)HPNikR and P<sub>ureA</sub> utilized an oligomer that was 49 bp in length which contained the recognition palindrome (23). This oligomer was chosen because it corresponds to the region that others had identified to be protected by Ni(II)HPNikR using DNase footprinting (19, 20, 22, 24). The ability of Ni(II)HPNikR to recognize shorter DNA sequences had not been determined, and we sought to ascertain whether Ni(II)HPNikR could recognize a shorter P<sub>ureA</sub> sequence. We examined the binding interaction between Ni(II)HPNikR and two shorter sequences: a 32-oligonucleotide sequence, P<sub>ureA</sub>-32, and a 27-oligonucleotide sequence, P<sub>ureA</sub>-27. Both oligomers contained the asymmetric recognition palindrome. Ni(II)HPNikR bound P<sub>ureA</sub>-32 tightly with a  $K_d$  of  $14 \pm 2.9 \text{ nM}$ , while Ni(II)HPNikR did not show any discernible binding to P<sub>ureA</sub>-27 (Figure 1b,c). P<sub>ureA</sub>-32 contains five additional oligonucleotides compared to P<sub>ureA</sub>-27 with an AT sequence at the 5' end and a TTA sequence at the 3' end. To test whether the recognition of P<sub>ureA</sub>-32 but not P<sub>ureA</sub>-27 by Ni(II)HPNikR is due to sequence specific binding to the additional five oligonucleotides, the binding interaction between Ni(II)HPNikR and a mutant of P<sub>ureA</sub>-32 called P<sub>ureA</sub>-32GC in which the five additional AT rich oligonucleotides

Table 2

unlabeled DNA	$K_d$ (nM)	unlabeled DNA	$K_d$ (nM)
P <sub>ureA</sub> -49	$67 \pm 1.0$	P <sub>ureA</sub> -perf	$143 \pm 10$
P <sub>ureA</sub> -Δpal	no binding	P <sub>ureA</sub> -32	$14 \pm 2.9$
P <sub>ureA</sub> -Δpal1	$1000 \pm 94$	P <sub>ureA</sub> -32GC	$11 \pm 3.6$
P <sub>ureA</sub> -Δpal2	$4900 \pm 780$	P <sub>ureA</sub> -27	no binding

from P<sub>ureA</sub>-32 were modified to cytosines was studied. This mutant also exhibited a tight binding interaction with Ni(II)HPNikR, with a determined  $K_d$  of  $11 \pm 3.6 \text{ nM}$  (Figure 1b). Taken together, the results suggest that rather than a loss of base specific contacts, P<sub>ureA</sub>-27 fails to bind to Ni(II)HPNikR because it is too short to form a stable complex (Table 2 and Figure 1a,b).

Corresponding electrophoretic mobility gel shift assays demonstrating HPNikR binding to all of the P<sub>ureA</sub> variant sequences were also performed. These experiments, shown in Figure S2a (Supporting Information), confirmed the trends in binding affinities observed from the FA assays.

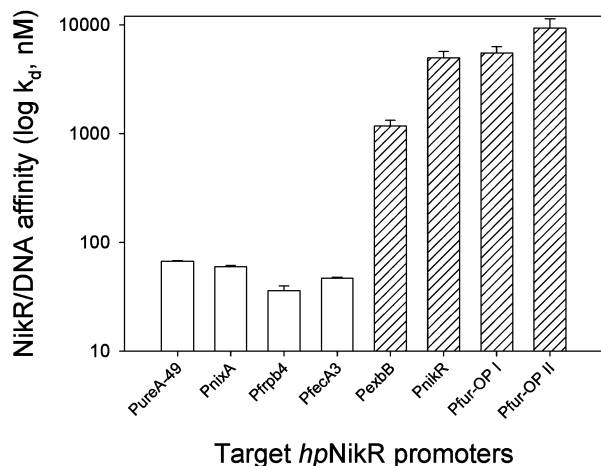
**Competitive Binding Titrations with Other Target Ni(II)HPNikR Promoters.** Ni(II)HPNikR has been shown to regulate the expression of multiple genes, including some involved in nickel ion homeostasis, iron regulation, and acid adaptation. For several of these target genes, DNase footprinting studies and/or electrophoretic gel mobility shift assays (EMSA) have been conducted to verify a direct binding role for Ni(II)HPNikR and to map the binding site within the respective promoter region (14, 19, 20, 22, 24, 25); however, the Ni(II)HPNikR binding affinities for most of these target promoters have yet to be elucidated.

We have undertaken a comprehensive binding analysis of the interaction between Ni(II)HPNikR and *ureA*, *nixA*, *fecA3*, *frpB4*, *exbB*, *nikR*, and *fur* promoters using competitive fluorescence anisotropy assays and electrophoretic mobility gel shift assays. With the aid of binding regions identified through previous studies, DNA promoter fragments composed of 49 bp were designed for each gene of interest (Figure 2a). Figure 2c displays representative competitive binding titrations for three of the sequences, P<sub>fecA3</sub>, P<sub>exbB</sub>, and P<sub>fur</sub>-OPI. The determined dissociation constants,  $K_d$ 's, for each sequence tested in this study are displayed graphically in Figure 2b and listed in Table 3. Five of the genes regulated are involved in nickel homeostasis. Ni(II)HPNikR bound the promoters of four of these genes very tightly, with determined dissociation constants,  $K_d$ , of  $67 \pm 1.0 \text{ nM}$  for *ureA*,  $60 \pm 1.6 \text{ nM}$  for *nixA*,  $47 \pm 4.1 \text{ nM}$  for *fecA3*, and  $36 \pm 4.5 \text{ nM}$  for *frpB4*. These results indicate that Ni(II)HPNikR tightly regulates the expression of these genes. Ni(II)HPNikR bound the *nikR* promoter with a significantly weaker affinity ( $K_d = 5.0 \pm 0.70 \mu\text{M}$ ). The operator region of genes associated with iron uptake and regulation, *exbB* and *fur* (two promoters, *furOPI* and *furOPII*), also exhibited weak binding to Ni(II)HPNikR with affinities of  $1.2 \pm 0.15$ ,  $5.5 \pm 0.79$ , and  $9.8 \pm 2.0 \mu\text{M}$ , respectively. Corresponding electrophoretic mobility gel shift assays demonstrating Ni(II)HPNikR binding to all of the additional target promoter sequences have also been performed. These experiments, shown in Figure S2b (Supporting Information), confirmed the trends in binding affinities observed from the FA assays.

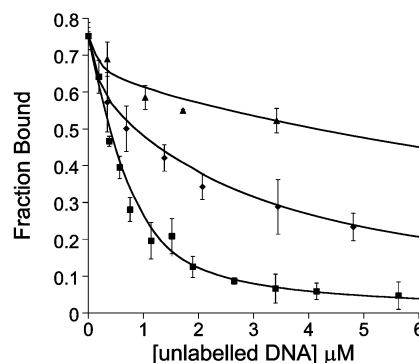
**Electrostatic Contribution to Ni(II)HPNikR–DNA Binding.** Titrations were performed at a range of ionic strengths to determine the influence of electrostatics on Ni(II)HPNikR–

*P<sub>ureA</sub>-F* (-95 to -47) CTTCAAAGATA **TAACACT** AATT **C**ATTTTAAATAATAATTAGTTAATGAA  
*P<sub>ureA</sub>-49* (-95 to -47) CTTCAAAGATA **TAACACT** AATT CATTTTAAATAATAATTAGTTAATGAA  
*P<sub>nixA</sub>* (-18 to +31) AACAAAATA **TATTACA** ATTACCAAAAAAGTATTATTTTCTTAAAAGGT  
*P<sub>frpB4</sub>* (-43 to -8) ACAAAATTTAAGG **TATTATT** AAATAGAATAATGTGAATAATAACCTTAGGT  
*P<sub>fecA3</sub>* (-7 to +31) TAAAATTCGCA **CATTATT** AAGTTTTTTTTGTTTTTATTACTTAATAAT  
*P<sub>exbB</sub>* (-37 to +1) TTATTGACTTGT **TATTATT** AAAACAATATAATCAACAACCAACATTCC  
*P<sub>nikR</sub>* (-27 to +10) AAATCCAGTTTG **TATTATA** ATTGTTCATTTTAAATTAATTCAATCATAC  
*P<sub>fur-OP I</sub>* (-24 to +1) TATGTTTCATCG **CATTATT** ATTGTATAATAATATTTCTAGTTATAAAAAAT  
*P<sub>fur-OP II</sub>* (-122 to -86) ATAAGAAATTGA **TCTTATA** AGTTACATTAAATGCGACAATGGTAATAA

(a)



(b)



(c)

FIGURE 2: Fluorescence anisotropy-monitored binding of NiHPNikR to target operator sequences. (a) Oligonucleotide sequences used in this study. The putative palindrome is boxed, and for *P<sub>ureA</sub>-F*, the fluorescently labeled thymine is highlighted with a black background. (b) Graphical representation of determined dissociation constants,  $K_d$ 's, observed for NiHPNikR with the protein target operator sequences. (c) Competitive titration of unlabeled *P<sub>fecA3</sub>* (49mer) (■) into 15 nM *P<sub>ureA</sub>-F* and 375 nM NikR and titrations of unlabeled *P<sub>exbB</sub>* (◆) and *P<sub>fur-OP I</sub>* (▲) into 5 nM *P<sub>ureA</sub>-F* and 88 nM NikR are shown.

Table 3

unlabeled DNA	$K_d$ (nM)	unlabeled DNA	$K_d$ (nM)
<i>P<sub>ureA</sub>-49</i>	67 ± 1.0	<i>P<sub>exbB</sub></i>	1200 ± 150
<i>P<sub>nixA</sub></i>	60 ± 1.6	<i>P<sub>nikR</sub></i>	5000 ± 700
<i>P<sub>frpB4</sub></i>	36 ± 4.5	<i>P<sub>fur-OP I</sub></i>	5500 ± 790
<i>P<sub>fecA3</sub></i>	47 ± 4.1	<i>P<sub>fur-OP II</sub></i>	9800 ± 2000

DNA binding. These studies were performed for the interaction between Ni(II)HPNikR and a “tight binder” DNA (*ureA-F*) and between Ni(II)HPNikR and a “weak binder” DNA (*furOP I*). The number of ions released during the interaction can be determined by plotting  $\log K_a$  versus  $\log[\text{NaCl}]$  and fitting the data to the equation  $\log K_a = \log K_{a,\text{net}} - Z\Psi \log[\text{NaCl}]$ .  $Z\Psi$  quantifies the number of ions released upon protein–DNA binding (32–34) (Figure 3). For the Ni(II)HPNikR–*pUreA-F* interaction, ~4 ions (4.4) were released upon protein–DNA association. For the Ni(II)HPNikR–*pFur-OP I* interaction, ~4 ions (3.5) were released. These results suggest that there is a similar electrostatic component to binding for both the tight and weak binders.

**Mg, Ca, and Mn Dependence of DNA Binding.** For Ni(II)HPNikR–*pUreA* binding to occur, a second “low-affinity” metal ion [Mg, Ca, or Mn(II)] must be present. All FA studies were performed with 3 mM magnesium chloride in the buffer based on our previous report that showed maximal Ni(II)HPNikR–DNA binding at this Mg concen-

tration (23). To quantify the dependence on the low-affinity metal ions, the Ni(II)HPNikR–DNA complex was titrated with each of the three low-affinity metal ions and the fluorescence anisotropy monitored. The binding isotherms were fit to a 1:1 binding model, and dissociation constants ( $K_d$ 's) of 390 ± 13 μM for Mg, 510 ± 92 μM for Ca, and 20 ± 2 μM for Mn(II) were determined.

**Requirement of Magnesium in DNA Recognition.** All of our studies on the low-affinity metal ion have focused on the interaction of Ni(II)HPNikR with *ureA* (23). Chivers and co-workers observed a similar low-affinity metal ion effect for *nixA* binding using an EMSA (20). To determine if this magnesium requirement is operative for the additional gene promoters studied here, gel shift assays in which magnesium was excluded from the buffer were performed. Ni(II)HPNikR did not exhibit binding to any of the target promoters in the absence of magnesium, indicating a general requirement of magnesium for HPNikR–DNA binding (Figure S2 of the Supporting Information).

## DISCUSSION

Ni(II)HPNikR directly and indirectly regulates the transcription of a large group of genes that are essential for the survival of the organism (12). Each of the eight genes currently known to be directly regulated by Ni(II)HPNikR contains a slightly different pseudopalindromic recognition

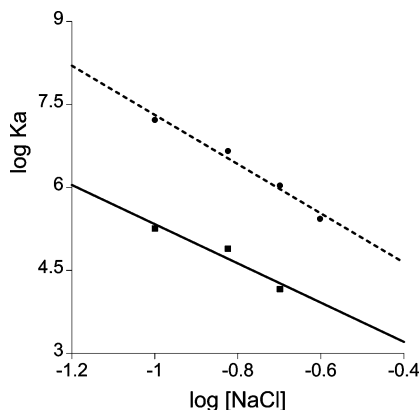


FIGURE 3: Plot of the dependence of the logarithm of the association constant ( $K_a$ ) of Ni(II)NikR with the *pUreA* (●) and *pFur OPI* (■) sequences as a function of the logarithm of the NaCl concentration.

sequence, and it is not apparent how Ni(II)*HPNikR* can distinguish between these different promoter sequences (Figure 2a). We have undertaken studies of the binding interactions between Ni(II)*HPNikR* and the genes that the protein directly regulates to address the question of how *HPNikR* recognizes and distinguishes between these genes (19–22, 24, 25). Using a competitive fluorescence anisotropy assay, we have examined the role of the recognition palindrome and sequence length in the Ni(II)*HPNikR*–DNA binding interaction. Prior to our studies, we hypothesized that Ni(II)*HPNikR* would exhibit differential binding affinities for the eight recognition sequences as part of a mechanism employed by Ni(II)*HPNikR* to distinguish between the various genes it regulates in vivo. Surprisingly, by quantifying these interactions, we discovered that Ni(II)*HPNikR* binds to its target promoter sequences with either high or low affinity. We now propose a two-tiered DNA recognition model.

We had previously shown that Ni(II)*HPNikR* binds to the *ureA* promoter,  $P_{ureA}$ , with nanomolar affinity and that the pseudopalindromic recognition site was absolutely required for binding (23). Here, we evaluated the role of each subsite of the  $P_{ureA}$  recognition palindrome in protein recognition by altering the sequence of each site to all cytosines and measuring the effect of the mutations on protein affinity (Figure 1a). Both mutants exhibited decreased DNA binding affinity, suggesting that the integrity of both subsites of the palindrome is essential for *ureA* recognition. Modification of the second subsite of the palindrome had a moderately greater effect on *HPNikR* binding affinity than modification of the first, indicating that this half-site plays a larger role in protein recognition. The large decreases in binding affinity that occur when either half-site is removed via sequence modification suggest that binding to both sites is cooperative.

Ni(II)*HPNikR* is a member of the ribbon–helix–helix transcription factor family (35, 36), members of which typically recognize symmetrical DNA operator sequences, such as in *ECNikR* (28, 37), *Arc* (38), and *MetJ* (39). Our studies revealed that *HPNikR* does not preferentially bind to a symmetrical DNA operator sequence: *HPNikR* shows a weaker affinity for the “perfect”  $P_{ureA}$  palindrome ( $P_{ureA-perf}$ ), with the repeat, TATTATT-X<sub>11</sub>-AATAATA (Figure 1a), than for the native, nonsymmetrical wild-type operator ( $P_{ureA}$ ). We propose that either *HPNikR* has no real preference for

a perfect palindrome and that it readily binds to an asymmetric recognition site as long as certain key nucleotides are present or the predicted recognition palindrome is not optimal for Ni(II)*HPNikR* binding and another more potent palindrome repeat exists. It is notable that for all of the identified *HPNikR* target genes, all of the recognition binding sites are asymmetric.

The  $P_{ureA}$  recognition sequence is made up of 49 bp and corresponds to the region protected in DNase footprinting assays (19, 20, 22, 24). Within this sequence is the pseudopalindromic recognition site consisting of seven bases per subsite. Studies examining the length of  $P_{ureA}$  required for *HPNikR* recognition revealed that in addition to the palindrome, five flanking nucleotides are required for a stable complex to be formed. The sequence of these flanking nucleotides could be altered without any effect on binding affinity, and we propose that *HPNikR* makes critical nonspecific phosphate backbone interactions with these additional flanking residues. Such interactions with the DNA phosphate backbone were seen in a recently determined *E. coli* NikR–DNA crystal structure (37).

By systematically measuring the affinity of *HPNikR* for each of the genes it directly regulates, *ureA*, *nixA*, *fecA3*, *frpB4*, *exbB*, *nikR*, and *fur OPI* and *fur OPII*, we sought to define the hierarchical importance of the genes within the *HPNikR* regulon. We determined that *HPNikR* bound to four sequences, *ureA*, *nixA*, *fecA3*, and *frpB4*, with nanomolar affinity and to four others, *exbB*, *nikR*, *fur OPI*, and *fur OPII*, with micromolar affinity. We propose that this two-tiered level of recognition can be explained in the context of these genes’ physiological roles.

The four genes that *HPNikR* binds tightly are all involved in nickel uptake and processing. One of these genes, *ureA*, which encodes the enzyme urease is activated by *HPNikR*. Nickel-bound urease functions to convert urea to ammonia and bicarbonate which are then released by the cell to neutralize the local microenvironment (8, 9). *H. pylori* requires high levels of urease to contend with high intracellular nickel concentrations and the low pH of its local environment (14, 40). Because *HPNikR* is an activator of *ureA* transcription, the observed tight binding interaction between *HPNikR* and *ureA* is in keeping with *H. pylori*’s requirement for high levels of urease (19, 20, 23).

The three remaining genes that *HPNikR* bind tightly, *NixA*, *FecA3*, and *FrpB4*, are all involved in nickel uptake and are repressed by *HPNikR*. *NixA* is an inner membrane nickel permease (8, 15, 24), and *FecA3* and *FrpB4* are nickel specific outer membrane importers (25, 41). The high affinities of *HPNikR* for the promoters of *NixA*, *FecA3*, and *FrpB4* are in keeping with the immediate requirement that the *H. pylori* organism shut off the acquisition of nickel during periods in which levels of intracellular nickel are elevated.

One of the promoters that Ni(II)*HPNikR* binds to weakly, *exbB*, provides energy for nickel import via *FecA3/FrpB4* as the *exbB*–*exbD*–*tonB* (*HP1339*–*1440*–*1441*) protein complex (25, 41). The *exbB*–*exbD*–*tonB* protein complex does not function solely to supply energy for nickel uptake; for instance, iron import also requires the *exbB2*–*exbD2*–*tonB* energy machinery (41) with the iron regulatory protein *HPFur* controlling *exbB*–*exbD*–*tonB* transcription. We propose that the weak regulation of *exbB*–*exbD*–*tonB* by



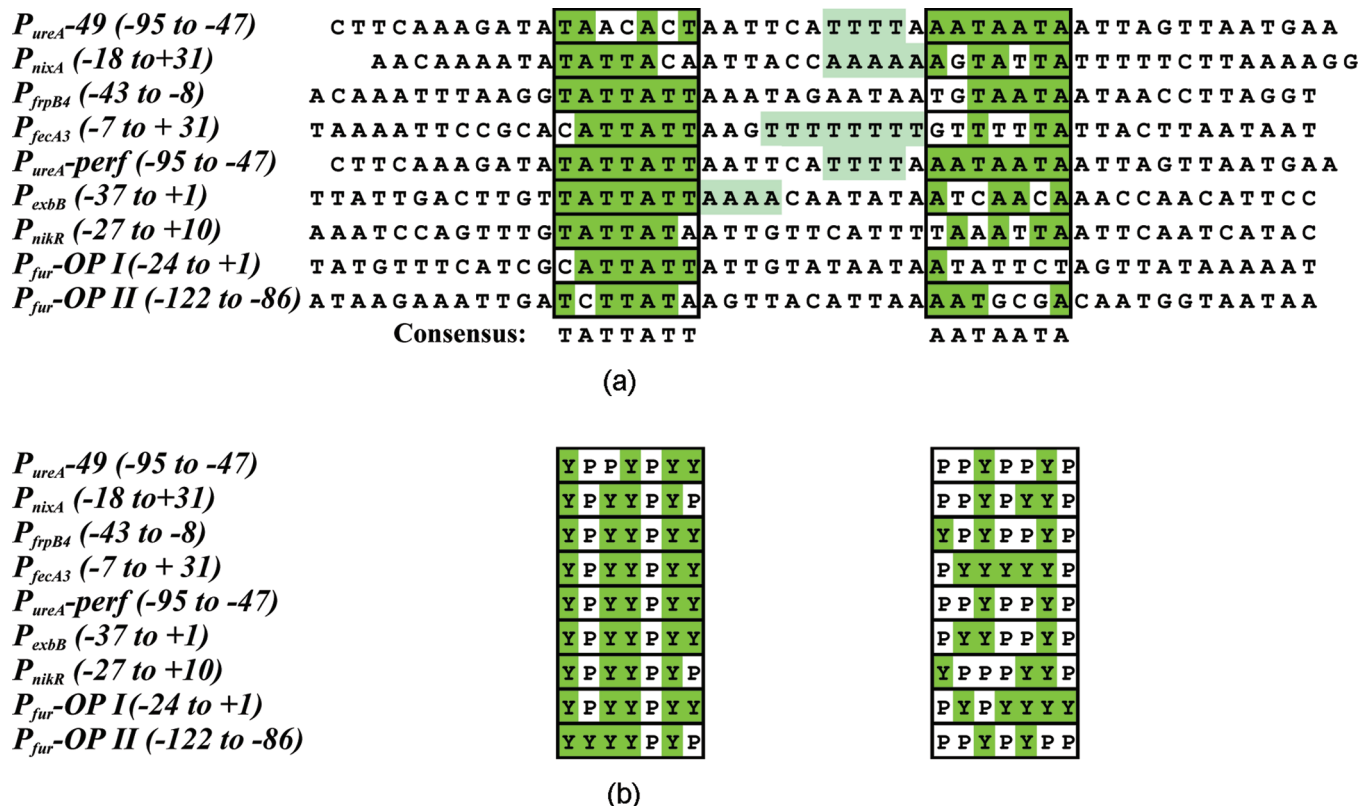


FIGURE 4: Alignment of target NiHPNikR operator binding sites. (a) The putative palindrome regions, based on that determined for the *ureA* operator, are boxed in black. Conserved bases are highlighted in green with the proposed palindrome shown below. Regions within the spacer containing “AT tracts” are highlighted in light green. (b) The purine (P) and pyrimidine (Y) composition of the subsites is shown compiled for the target NikR operators.

HPNikR may be due to the dual repressive nature of NikR and Fur at this promoter. It would be detrimental to the import of iron if the *exbB*-*exbD*-*tonB* system was too readily shut off by the presence of nickel and HPNikR.

HPNikR also binds weakly to the *nikR* promoter which encodes HPNikR. HPNikR acts as a repressor of this gene (12, 19, 20, 22). Because HPNikR regulates multiple genes under normal cellular conditions, we propose that weak repression of *nikR* by HPNikR allows HPNikR to fulfill its large range of functions. There are two previous reports of HPNikR binding to its own promoter. Zamble and co-workers used EMSA assays to report that HPNikR binds to its promoter, and they noted that substantially higher concentrations of HPNikR are required to elicit DNA binding to the *NikR* promoter when compared to the *ureA* promoter, suggesting a weaker binding interaction for HPNikR and *nikR* compared to HPNikR and *ureA*. Chivers and co-workers reported a  $K_d$  of 120 nM for the HPNikR-*nikR* interaction using gel shift assays (20). The discrepancies in the  $K_d$  values obtained in these reports may reflect the differences in the techniques employed as well as the experimental conditions (which included different length DNA fragments and different concentrations of metal ions). Our results favor a model, also proposed by Zamble and co-workers, in which the transcription of HPNikR is only autorepressed when intracellular levels of nickel-bound HPNikR have reached a high concentration threshold where additional levels of HPNikR are no longer necessary.

We have also determined that HPNikR weakly regulates *fur* by binding weakly to two sites in the promoter: *OPI* and *OPII* (22). The transcriptional role of HPNikR at the *fur*

promoter is unresolved. The *OPI* site covers nucleotides -24 to +1 which overlaps the -10 hexameric element of the *fur* promoter, suggesting that HPNikR is a transcriptional repressor (22). The *OPII* site is found well upstream of the transcriptional start, spanning nucleotides -122 to -86 (22). Typically, proteins that bind upstream of the transcription machinery are activators that recruit proteins or modulate a repressive nature of the DNA, suggesting that HPNikR might be an activator at this site. Chivers and co-workers reported a tighter  $K_d$  using DNase footprinting studies, and again the discrepancy may be due to differences in technique and conditions (20).

Ni(II)HPNikR requires the presence of a second metal ion [Mg, Ca, or Mn(II)] for DNA binding to be observed by fluorescence anisotropy or an EMSA (20, 23), although not by ITC (42). We determined that these metal ions have weak affinities (micromolar) for Ni(II)HPNikR in the presence of *ureA*. Zambelli and co-workers recently reported a low-affinity metal binding site in Ni(II)HPNikR occupied by nickel (43). The affinity of nickel for this low-affinity site is 500  $\mu$ M. This affinity is in the same regime as the affinities we measured for Mg, Ca, and Mn(II) binding to HPNikR, and we speculate that all four metal ions may occupy the same low-affinity site.

The presence of a high-affinity metal binding site and a low-affinity metal binding site in HPNikR brings up the question of which metal ion controls HPNikR function. The total concentrations of the low-affinity metal ions in *H. pylori* are not known; however, they can be inferred from levels measured in *E. coli* where Mg is present at >10 mM, Ca at ~0.1 mM, and Mn(II) at a micromolar level (18, 44). Given



these concentrations, the low-affinity sites on *HPNikR* are likely populated under normal physiological conditions, suggesting that it is nickel availability for binding to the high-affinity site that controls *HPNikR* function. The two-tiered binding model that we propose here suggests that total nickel, total *HPNikR*, or both total nickel and total *HPNikR* fluctuate in the cell to modulate regulation. Nickel availability in *H. pylori* has been shown to control urease and NixA expression levels, lending support to a model that includes fluctuating nickel levels controlling function (14, 15, 45). The variability of *HPNikR* concentrations in *H. pylori* has not been reported, and work is in progress to measure these concentrations as variability in these levels may also drive the two-tiered recognition effect.

From a sequence level, we can also draw some distinctions between the tight and weak binders. Figure 4a shows the promoter sequences tested in this study aligned with direct matches to the putative palindrome TATTATT-X<sub>11</sub>-AATAA-TA highlighted. The absence of a classical symmetric recognition palindrome may help explain why a range binding affinities is observed. The first subsite shows a high degree of sequence conservation and resembles the proposed consensus sequence. In contrast, the second subsite shows less sequence conservation and, apart from the *ureA* operator, very loosely resembles the proposed consensus sequence. Figure 4b shows the purine (P) and pyrimidine (Y) composition of the compiled promoters. The first subsite shows a more highly conserved purine and pyrimidine composition than the second subsite. On the basis of the greater degree of sequence conservation in the first subsite, we propose that sequence elements within the second subsite dictate the binding strength of individual promoters as this subsite has considerable sequence variation. Our experimental evidence that the removal of the second subsite has a greater effect on NikR–DNA binding affinity than removal of the first supports this hypothesis. We also point out that in the second palindrome, thymine residues at positions 10 and 13 are absolutely conserved among the tight binding promoters (*ureA*, *nixA*, *fecA3*, and *frpB4*) but are largely absent from the weak binding promoters (*nikR* and *fur*), suggesting that thymine residues may be important. Interestingly, in the X-ray structure of *E. coli* NikR bound to *NikA*, thymine residues are directly involved in interactions with the protein side chains from residues Arg3 and Thr5 (37). These residues are conserved in the *HPNikR* sequence (Arg 12 and Ser14), suggesting that *HPNikR* may make similar thymine specific contacts with DNA. Work to address the role of specific bases in *HPNikR*–DNA recognition is ongoing.

## ACKNOWLEDGMENT

We thank our colleagues in the Michel laboratory as well as the Wilks and Pozharskiy laboratories for helpful comments.

## SUPPORTING INFORMATION AVAILABLE

Competitive titrations of unlabeled DNA into PureA-F and NikR (Figure S1), EMSAs between Ni*HPNikR* and P<sub>ureA</sub><sup>−</sup>49, P<sub>ureA</sub>−Δ<sub>pal</sub>, P<sub>ureA</sub>−Δ<sub>pal1</sub>, P<sub>ureA</sub>−Δ<sub>pal2</sub>, P<sub>ureA</sub>−per<sub>f</sub>, P<sub>ureA</sub>−32, P<sub>ureA</sub>−32GC, and P<sub>ureA</sub>−27 (Figure S2a), EMSAs between Ni*HPNikR* and P<sub>ureA</sub>, P<sub>nixA</sub>, P<sub>fecA3</sub>, P<sub>frpB4</sub>, P<sub>exbB</sub>, P<sub>nikR</sub>, P<sub>fur</sub>−*OPI*, and P<sub>fur</sub>−*OPII* (Figure S2b), EMSAs of Ni(II)*HPNikR* and DNA in the absence of 3 mM MgCl<sub>2</sub> (Figure S2c), and titrations of

MgCl<sub>2</sub>, CaCl<sub>2</sub>, and MnCl<sub>2</sub> with [Ni(II)*HPNikR*]<sub>4</sub>/p*UreA*-F fit to 1:1 binding site model (Figure S3). This material is available free of charge via the Internet at <http://pubs.acs.org>.

## REFERENCES

- Marshall, B. J., and Warren, J. R. (1984) Unidentified curved bacilli in the stomach of patients with gastritis and peptic ulceration. *Lancet* 1, 1311–1315.
- Kusters, J. G., van Vliet, A. H., and Kuipers, E. J. (2006) Pathogenesis of *Helicobacter pylori* infection. *Clin. Microbiol. Rev.* 19, 449–490.
- Cover, T. L., and Blaser, M. J. (1992) *Helicobacter pylori* and gastroduodenal disease. *Annu. Rev. Med.* 43, 135–145.
- Sepulveda, A. R., and Coelho, L. G. (2002) *Helicobacter pylori* and gastric malignancies. *Helicobacter* 7 (Suppl. 1), 37–42.
- Loughlin, M. F. (2003) Novel therapeutic targets in *Helicobacter pylori*. *Expert Opin. Ther. Targets* 7, 725–735.
- Bik, E. M., Eckburg, P. B., Gill, S. R., Nelson, K. E., Purdom, E. A., Francois, F., Perez-Perez, G., Blaser, M. J., and Relman, D. A. (2006) Molecular analysis of the bacterial microbiota in the human stomach. *Proc. Natl. Acad. Sci. U.S.A.* 103, 732–737.
- van Vliet, A. H., Kuipers, E. J., Stoof, J., Poppelaars, S. W., and Kusters, J. G. (2004) Acid-responsive gene induction of ammonia-producing enzymes in *Helicobacter pylori* is mediated via a metal-responsive repressor cascade. *Infect. Immun.* 72, 766–773.
- Mobley, H. L., Island, M. D., and Hausinger, R. P. (1995) Molecular biology of microbial ureases. *Microbiol. Rev.* 59, 451–480.
- Mulrooney, S. B., and Hausinger, R. P. (2003) Nickel uptake and utilization by microorganisms. *FEMS Microbiol. Rev.* 27, 239–261.
- Stingl, K., and De Reuse, H. (2005) Staying alive overdosed: How does *Helicobacter pylori* control urease activity? *Int. J. Med. Microbiol.* 295, 307–315.
- Krishnaswamy, R., and Wilson, D. B. (2000) Construction and characterization of an *Escherichia coli* strain genetically engineered for Ni(II) bioaccumulation. *Appl. Environ. Microbiol.* 66, 5383–5386.
- Contreras, M., Thiberge, J. M., Mandrand-Berthelot, M. A., and Labigne, A. (2003) Characterization of the roles of NikR, a nickel-responsive pleiotropic autoregulator of *Helicobacter pylori*. *Mol. Microbiol.* 49, 947–963.
- Dosanjh, N. S., and Michel, S. L. (2006) Microbial nickel metalloregulation: NikRs for nickel ions. *Curr. Opin. Chem. Biol.* 10, 123–130.
- van Vliet, A. H., Poppelaars, S. W., Davies, B. J., Stoof, J., Bereswill, S., Kist, M., Penn, C. W., Kuipers, E. J., and Kusters, J. G. (2002) NikR mediates nickel-responsive transcriptional induction of urease expression in *Helicobacter pylori*. *Infect. Immun.* 70, 2846–2852.
- Wolfram, L., Haas, E., and Bauerfeind, P. (2006) Nickel represses the synthesis of the nickel permease NixA of *Helicobacter pylori*. *J. Bacteriol.* 188, 1245–1250.
- Giedroc, D. P., and Arunkumar, A. I. (2007) Metal sensor proteins: Nature's metalloregulated allosteric switches. *Dalton Trans.*, 3107–3120.
- Totter, S., Harvie, D. R., and Robinson, N. J. (2005) Understanding how cells allocate metals using metal sensors and metallochaperones. *Acc. Chem. Res.* 38, 775–783.
- Finney, L. A., and O'Halloran, T. V. (2003) Transition metal speciation in the cell: Insights from the chemistry of metal ion receptors. *Science* 300, 931–936.
- Abraham, L. O., Li, Y., and Zamble, D. B. (2006) The metal- and DNA-binding activities of *Helicobacter pylori* NikR. *J. Inorg. Biochem.* 100, 1005–1014.
- Benanti, E. L., and Chivers, P. T. (2007) The N-terminal arm of the *Helicobacter pylori* Ni<sup>2+</sup>-dependent transcription factor NikR is required for specific DNA binding. *J. Biol. Chem.* 282, 20365–20375.
- Davis, G. S., Flannery, E. L., and Mobley, H. L. (2006) *Helicobacter pylori* HP1512 is a nickel-responsive NikR-regulated outer membrane protein. *Infect. Immun.* 74, 6811–6820.
- Delany, I., Ieva, R., Soragni, A., Hillerigmann, M., Rappuoli, R., and Scarlato, V. (2005) In vitro analysis of protein-operator interactions of the NikR and Fur metal-responsive regulators of coregulated genes in *Helicobacter pylori*. *J. Bacteriol.* 187, 7703–7715.

23. Dosanjh, N. S., Hammerbacher, N. A., and Michel, S. L. J. (2007) Characterization of the *Helicobacter pylori* NikR-P(ureA) DNA interaction: Metal ion requirements and sequence specificity. *Biochemistry* 46, 2520–2529.
24. Ernst, F. D., Kuipers, E. J., Heijens, A., Sarwari, R., Stoof, J., Penn, C. W., Kusters, J. G., and van Vliet, A. H. (2005) The nickel-responsive regulator NikR controls activation and repression of gene transcription in *Helicobacter pylori*. *Infect. Immun.* 73, 7252–7258.
25. Ernst, F. D., Stoof, J., Horrevoets, W. M., Kuipers, E. J., Kusters, J. G., and van Vliet, A. H. (2006) NikR mediates nickel-responsive transcriptional repression of the *Helicobacter pylori* outer membrane proteins FecA3 (HP1400) and FrpB4 (HP1512). *Infect. Immun.* 74, 6821–6828.
26. Tomb, J. F., White, O., Kerlavage, A. R., Clayton, R. A., Sutton, G. G., Fleischmann, R. D., Ketchum, K. A., Klenk, H. P., Gill, S., Dougherty, B. A., Nelson, K., Quackenbush, J., Zhou, L., Kirkness, E. F., Peterson, S., Loftus, B., Richardson, D., Dodson, R., Khalak, H. G., Glodek, A., McKenney, K., Fitzgerald, L. M., Lee, N., Adams, M. D., Hickey, E. K., Berg, D. E., Gocayne, J. D., Utterback, T. R., Peterson, J. D., Kelley, J. M., Cotton, M. D., Weidman, J. M., Fujii, C., Bowman, C., Watthey, L., Wallin, E., Hayes, W. S., Borodovsky, M., Karp, P. D., Smith, H. O., Fraser, C. M., and Venter, J. C. (1997) The complete genome sequence of the gastric pathogen *Helicobacter pylori*. *Nature* 388, 539–547.
27. van Vliet, A. H., Ernst, F. D., and Kusters, J. G. (2004) NikR-mediated regulation of *Helicobacter pylori* acid adaptation. *Trends Microbiol.* 12, 489–494.
28. Chivers, P. T., and Sauer, R. T. (2000) Regulation of high affinity nickel uptake in bacteria.  $\text{Ni}^{2+}$ -dependent interaction of NikR with wild-type and mutant operator sites. *J. Biol. Chem.* 275, 19735–19741.
29. Rowe, J. L., Starnes, G. L., and Chivers, P. T. (2005) Complex transcriptional control links NikABCDE-dependent nickel transport with hydrogenase expression in *Escherichia coli*. *J. Bacteriol.* 187, 6317–6323.
30. De Pina, K., Desjardin, V., Mandrand-Berthelot, M. A., Giordano, G., and Wu, L. F. (1999) Isolation and characterization of the nikR gene encoding a nickel-responsive regulator in *Escherichia coli*. *J. Bacteriol.* 181, 670–674.
31. Lakowicz, J. R. (1999) *Principles of Fluorescence Spectroscopy*, 1st ed., Kluwer Academic/Plenum Publishers, New York.
32. Record, M. T., Jr., Anderson, C. F., and Lohman, T. M. (1978) Thermodynamic analysis of ion effects on the binding and conformational equilibria of proteins and nucleic acids: The roles of ion association or release, screening, and ion effects on water activity. *Q. Rev. Biophys.* 11, 103–178.
33. Lane, A. N., and Jenkins, T. C. (2000) Thermodynamics of nucleic acids and their interactions with ligands. *Q. Rev. Biophys.* 33, 255–306.
34. Dragan, A. I., Frank, L., Liu, Y., Makeyeva, E. N., Crane-Robinson, C., and Privalov, P. L. (2004) Thermodynamic signature of GCN4-bZIP binding to DNA indicates the role of water in discriminating between the AP-1 and ATF/CREB sites. *J. Mol. Biol.* 343, 865–878.
35. Chivers, P. T., and Sauer, R. T. (1999) NikR is a ribbon-helix-helix DNA-binding protein. *Protein Sci.* 8, 2494–2500.
36. Schreiter, E. R., and Drennan, C. L. (2007) Ribbon-helix-helix transcription factors: Variations on a theme. *Nat. Rev. Microbiol.* 5, 710–720.
37. Schreiter, E. R., Wang, S. C., Zamble, D. B., and Drennan, C. L. (2006) NikR-operator complex structure and the mechanism of repressor activation by metal ions. *Proc. Natl. Acad. Sci. U.S.A.* 103, 13676–13681.
38. Raumann, B. E., Rould, M. A., Pabo, C. O., and Sauer, R. T. (1994) DNA recognition by  $\beta$ -sheets in the Arc repressor-operator crystal structure. *Nature* 367, 754–757.
39. Spector, S., Sauer, R. T., and Tidor, B. (2004) Computational and experimental probes of symmetry mismatches in the Arc repressor-DNA complex. *J. Mol. Biol.* 340, 253–261.
40. Bauerfeind, P., Garner, R., Dunn, B. E., and Mobley, H. L. (1997) Synthesis and activity of *Helicobacter pylori* urease and catalase at low pH. *Gut* 40, 25–30.
41. Schauer, K., Gouget, B., Carriere, M., Labigne, A., and de Reuse, H. (2007) Novel nickel transport mechanism across the bacterial outer membrane energized by the TonB/ExbB/ExbD machinery. *Mol. Microbiol.* 63, 1054–1068.
42. Zambelli, B., Danielli, A., Romagnoli, S., Neyroz, P., Ciurli, S., and Scarlato, V. (2008) High-affinity  $\text{Ni}^{2+}$  binding selectively promotes binding of *Helicobacter pylori* NikR to its target urease promoter. *J. Mol. Biol.* 383, 1129–1143.
43. Zambelli, B., Bellucci, M., Danielli, A., Scarlato, V., and Ciurli, S. (2007) The  $\text{Ni}^{2+}$  binding properties of *Helicobacter pylori* NikR. *Chem. Commun.*, 3649–3651.
44. Outten, C. E., Tobin, D. A., Penner-Hahn, J. E., and O'Halloran, T. V. (2001) Characterization of the metal receptor sites in *Escherichia coli* Zur, an ultrasensitive zinc(II) metalloregulatory protein. *Biochemistry* 40, 10417–10423.
45. van Vliet, A. H., Kuipers, E. J., Waidner, B., Davies, B. J., de Vries, N., Penn, C. W., Vandenbroucke-Grauls, C. M., Kist, M., Bereswill, S., and Kusters, J. G. (2001) Nickel-responsive induction of urease expression in *Helicobacter pylori* is mediated at the transcriptional level. *Infect. Immun.* 69, 4891–4897.

BI801481J